Journal of Constructional Steel Research 167 (2020) 105825

Contents lists available at ScienceDirect

Journal of Constructional Steel Research

journal homepage: www.elsevier.com/locate/ijcard

Retrofitting of steel beams using low-modulus carbon fiber reinforced polymer laminates

Sivaganesh Selvaraj, Mahendrakumar Madhavan*

Department of Civil Engineering, Indian Institute of Technology Hyderabad, Kandi, Sangareddy, 502 285, Telangana, India

ARTICLE INFO

Article history:
Received 31 July 2019
Received in revised form
12 October 2019
Accepted 21 October 2019
Available online 20 December 2019

Keywords:
Retrofitting
Low-modulus CFRP
Feasibility study
Wrapping optimization
Design limit states

ABSTRACT

A feasibility study on the use of low modulus (<125 GPa) carbon fiber reinforced polymer (CFRP) in the retrofitting schemes of structural steel beams subjected to flexural loading is presented. A various CFRP wrapping optimization methods were introduced namely tension flange strengthening and U-wrap strengthening. The result indicates that the strength of the member can be increased significantly by adopting the appropriate wrapping method. A simple theoretical calculation to estimate the design moment capacity of the CFRP strengthened steel member with the nonlinear material properties has been presented. Further, the design stress and strain values recommended in the current design provisions of ACI were validated with the test results and found to be unconservative. Therefore, a method to evaluate the design strain of a strengthened structural steel member using low modulus CFRP has been suggested from the present results. The reliability study based on the limited test results also indicates that the suggested elastic strain design limit state is reliable. For ease of understanding, a design example for predicting the design strength of the steel flexural member strengthened using low modulus CFRP has been provided.

1. Introduction and background

The need for an in-situ method to rehabilitate and or retrofit the existing steel structural member such as main floor beam and lateral floor beam in structures that are subjected to flexural loading has increased significantly due to the increase in the live load magnitudes. The conventional retrofitting method using steel plate is not a viable solution due to heavyweight, difficulty in fixing and welding issues [1]. Though a new retrofitting method was developed using light gauge steel channels, it was concluded that the more robust design formulation is required for the implementation (Selvaraj and Madhavan 2019). One material that can substantially increase the strength and stiffness of the structural member without increasing the dead load on the structures is the fiber reinforced polymer (FRP). FRP's have been used in the aerospace and defense applications since the 1960s and the construction industry since the 1980s but did not gain widespread acceptance since they were expensive at the time of invention. However, in the last decade, the use of FRP in the infrastructure and construction sector has significantly increased due to its flexibility in the form (fabric, sheet, and plate) and strength [2–6]. The various CFRP retrofitting schemes for the flexural members used in the past has been graphically illustrated in Fig. 1.

The FRP's can be classified as low or normal modulus (with E_{CFRP} between 100 and 250 GPa) and high modulus (with E_{CFRP} greater than 250 GPa) [4]. The high modulus CFRP's (>250 GPa) are not typically available for common civilian applications in south Asian countries like India, though there is a tremendous need for infrastructural retrofitting. The present study, therefore, aims to develop an effective retrofitting method by using low modulus CFRP's (<125 GPa) through FRP wrapping optimization. It should be noted that very low modulus CFRP's (E = 66.6 GPa) that is not classified in Zhao and Zhang [4] is also used in the present study for investigation.

1.1. Need of a design method

In addition, the design provisions currently available for the design of FRP strengthened structural members for flexure [9–14]; and [1] is applicable only for the FRP materials that exhibit linear stress-strain response until failure, and does not cover the low modulus FRP fabrics or sheets that have multilinear stress-strain curves. Although the previous design provisions [1,13] suggests limiting the design strain to preclude debonding or plastification, it

* Corresponding author.
E-mail addresses: ce13p1009@iith.ac.in (S. Selvaraj), mkm@iith.ac.in (M. Madhavan).

https://doi.org/10.1016/j.jcsr.2019.105825
0143-974X/

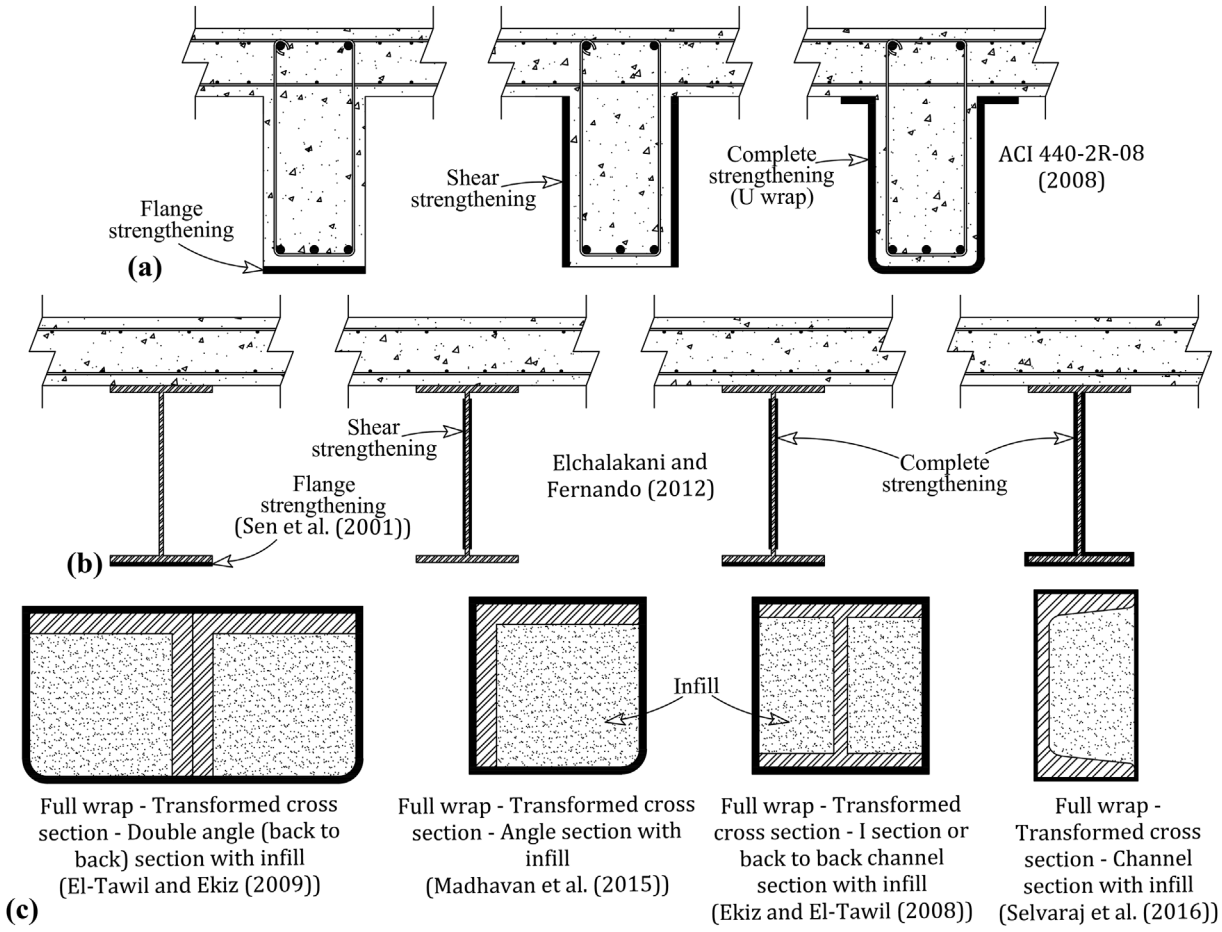

Fig. 1. Various FRP retrofitting schemes for flexural members: (a) For concrete structures (ACI 440.2R-08 (2008)); (b) For steel (Elchalakani and Fernando (2012)) and steel-concrete structures (Sen et al. (2001)); (c) For steel structures (cross-section transformation technique) (El-Tawil and Ekiz (2009) [7]; Ekiz and El-Tawil (2008) and [8].

does not provide specific design limit states for various modulus of CFRPs. The low modulus CFRP laminates were used for the strengthening of structural steel members for various loading conditions [5,15–18] [7,8,19–22] and [23,24]; Ghafoori et al., 2019; [25,26], however, no design works were attempted to investigate the suitability of the current ACI [13] design guidelines for CFRP retrofitted steel C channels.

Schnerch et al. [27] and Schnerch and Rizkalla [28] used the design provisions of ACI [13] for the design of steel-concrete composite beam strengthened using high-modulus CFRP. The results indicate that the design stress limitations recommended by ACI [13] are conservative. However, as per the authors' knowledge, the ACI [13] recommendations were not investigated for the design of beams strengthened using low-modulus CFRP's that exhibit multi-linear stress-strain material behavior. The present research work endeavors to bridge this gap.

In the present work, a feasibility of the use of low modulus CFRP laminates (<125 GPa) for the strengthening of steel beam is explored (Fig. 2). Though, the design calculation method used in this study may appears to be a simple sectional-analysis, the novelty of the work lies in the selection of the design limit state. The material property of the low modulus CFRP laminates used in this present work is different (multilinear stress-strain response) from the previous works (linear stress-strain response). Therefore, the method to adopt the multilinear stress-strain response in the design is explained. More importantly, a suitability of the current ACI [13] design limit state is examined for the steel beams strengthened with low-modulus CFRP. Based on the observations, an alternative and conservative design limit state is suggested. The reliability calculations were carried out as per AASHTHO guidelines to check the suitability of the suggested limit state.

2. Description of the work

The structural steel members in the steel foot over bridges (without concrete composite cross-section - Fig. 2) requires strengthening due to the increase in pedestrian traffic is considered in the present study. The steel beams in the foot over railway bridges in India are typically shallow, C channels. The cross-section dimensions of the C channel (ISMC 100 - Indian Standard Medium weight Channel (ISMC) with a depth of 100 mm) used in this study were obtained from IS 808 [29]. The top flange connection of the secondary beams to the deck slab is typically made of intermittent spot welding or staggered intermittent welding. The top flange connection of the beams to the deck slab provides continuous lateral restraint which prevents the channel sections from twisting during loading. Therefore, the only possible mode of failure is due to yield. Hence, the steel channels are usually designed up to the yield moment capacity (M_y) with a partial safety factor for material (γ_{mo}) [30]) (Eq. (1)). A 6 mm steel plate at the top flange of the C channels were welded to simulate such a behavior (restraint in the top flange) as shown in Fig. 2b and c.

$$M_{d(s)} = \frac{\beta_b Z_p f_y}{\gamma_{m0}} \quad (1)$$

The design strength of the laterally restrained beam can be determined from Eq. (1), where $M_{d(S)}$ is the design moment for steel

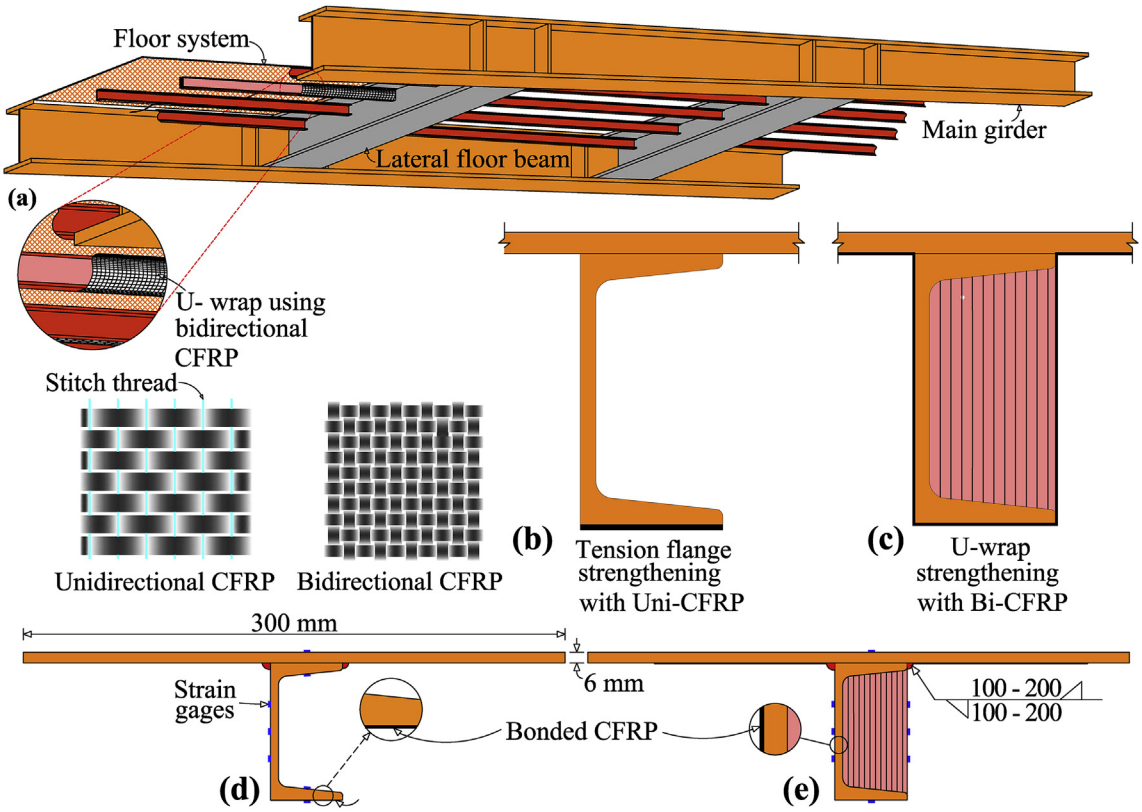

Fig. 2. (a) View of the structural steel member subjected to flexural loading; (b and c) CFRP strengthening technique used in the present work: Tension flange strengthening and U-wrap strengthening; (d and e) Position of strain gauges in the strengthened specimens.

beam as per IS 800 [30]; β_b is 1.0 for plastic/compact sections and $\beta_b = Z_e/Z_p$ for semi compact sections; Z_p is Plastic section modulus of the steel beam, Z_e is elastic section modulus of the steel beam; f_y is Yield stress obtained from the tensile test and γ_{mo} - Partial safety factor for material (governed by yielding). The design strength of the control beam (unstrengthened one) is calculated as follows:

Though the channel section ISMC 100 considered in this study is a plastic section as per table 2 of IS 800 [30]; the top plate attached to the channel top flange is a slender one as the outstanding element width to the thickness ratio (22.4) exceeds the limit (11.56) for the semi-compact section as per IS 800 [30]. Therefore, the test specimen (built-up section) is considered as a slender section, thereby the value of β_b in Eq. (1) is taken as equal to Z_e/Z_p. The values of the elastic section modulus (48.65×10^3 mm^3) and plastic section modulus (66×10^3 mm^3) are calculated for the built-up section (Fig. 2b) (ISMC 100 channel with top plate) and incorporated in Eq. (1). The yield strength of steel is taken as 346 MPa. Hence, the design moment of the built-up section is calculated as 15.30 kNm as per Eq. (1).

2.1. Proposed strengthening methods

Two different strengthening schemes namely tension flange strengthening and U-wrap (U shaped) strengthening using CFRP polymers were performed. Also, two different CFRP fabric types unidirectional fabric [HCU 232, 230 gsm (grams per square meter), 0.3 mm thick [31]] and bidirectional fabric [HCP 200C, 200 gsm, 0.2 mm thick [32]] were used in the strengthening schemes. Further, the strengthening schemes were divided into three and four configurations in tension flange strengthening and U-wrap strengthening schemes respectively by varying the number of strengthening layers. The tension flange strengthening schemes mean that the CFRPs were bonded only to the tension flange of the specimen (bottom flange of ISMC channel) as shown in Fig. 2b and U-wrap strengthening mean that the CFRP was wrapped in the U shape by enclosing the entire cross-section of the channel as shown (except top flange) in Fig. 2c. The strengthening approaches used in this present study is given in Table 1. It should be noted that a minimum of two CFRP layers was used in the present study since a single bidirectional CFRP wrap either in tension flange strengthening or closed wrapping provided insignificant strength improvement [7]. It should also be noted that the open side of the C channel was filled using a negligible stiffness infill material (cardboard) that acts as a formwork for the U shaped CFRP wrap. The core material cardboard used in this study is more vulnerable to crushing and crumbling than the other infill materials used by the former researchers [33,34] such as mortar, concrete, and wood. Such vulnerable behavior of cardboard brings more possibility for wrinkling failure in CFRP wrap, resulting in the need for identification of a robust wrapping configuration. The effect of moisture on the cardboard is validated in Selvaraj and Madhavan (2017). However, the possibility of moisture entrapment in the infill cardboard material is minimal since the test specimens are under the steel floor panel (Fig. 2). The objective of this study is focused primarily on the viability of adapting the low modulus CFRP as a repair technique for the strengthening of steel structures.

Four point bending tests were conducted for both the control (unstrengthened) and strengthened specimens. The increase in flexural strength of the member was determined by comparing the ultimate strength of the strengthened member to the control specimen. The out-to-out length of the test specimen is 2500 mm. More details on specimen fabrication and experimental test setup are given in the following sections.

Table 1
Summarized test results.

Specimen ID	Strengthening Scheme	Scheme definition	Exp. Max Moment (kNm)	Mean. Improvement in Strength (%)
Control	Tension flange strengthening (Fig. 2b)	–	20.72	–
T1U		One uni fabric in tension flange	23.19 20.93	6.50
T1U1B		One uni and bi fabric in tension flange	19.67 22.23	1.11
T2U1B		Two uni and bi fabric in tension flange	23.71 20.53	6.78
T1U + U1B	U-wrap strengthening (Fig. 2c)	Uni fabric in tension flange and one U shaped wrap by bi fabric	20.19 20.88	−0.86
T2U + U1B		Two uni fabric in tension flange and one U shaped wrap by bi fabric	27.02 26.55	29.30
T3U + U1B		Three uni fabric in tension flange and one U shaped wrap by bi fabric	25.00 27.24	26.09
T3U + U2B		Three uni fabric in tension flange and two U shaped wrap by bi fabric	28.70 31.63	45.62

Table 2
Results of design calculations.

Specimen	Exp. Ultimate moment (mean) M_{EXP} (kNm)	$M_{d\ (S)\ (IS\ 800)}$ (kNm) (bare steel specimen) Eq. (1)	Theoretical II Approach		Elastic strain method $M_{d\ (CS-\ \varepsilon E)}$ (kNm)	Improvement in design strength $M_{d\ (CS-\ \varepsilon E)}/M_{d\ (S)\ (IS\ 800)}$
			Ultimate stress method $M_{d\ (CS-\ \sigma U)}$ (kNm)	Ultimate strain method $M_{d\ (CS-\ \varepsilon U)}$ (kNm)		
T1U	22.06	15.30	21.91	22.65	16.65	1.09
T1U1B	20.95	15.30	22.15 0	23	16.77	1.10
T2U1B	22.12	15.30	23.20	24.5	17.09	1.12
T1U + U1B	20.54	15.30	22.22	23.03	16.90	1.10
T2U + U1B	26.79	15.30	23.26	24.53	17.22	1.13
T3U + U1B	26.12	15.30	24.32	26.04	17.55	1.15
T3U + U2B	30.17	15.30	24.62	26.43	17.79	1.16

2.2. Material properties

The mechanical properties of the materials in the composite cross-section were obtained from tensile tests for both steel (two specimens) and CFRP polymers (four specimens in each fabric type). The CFRP polymers for the tensile test specimens were fabricated with a resin content of 550 g per square meter of CFRP fabrics. The CFRP fabrics (both uni and bi) were layered one over another with resin coating for each layer to attain the required thickness for tensile testing. The wet CFRP polymers were rolled sufficiently to ensure a uniform thickness for the attachment of aluminum tabs. The dimensions of the tensile test specimens for steel, CFRP unidirectional and CFRP bidirectional fabrics are shown in Fig. 3a, b, and 3c respectively. The tensile test specimen

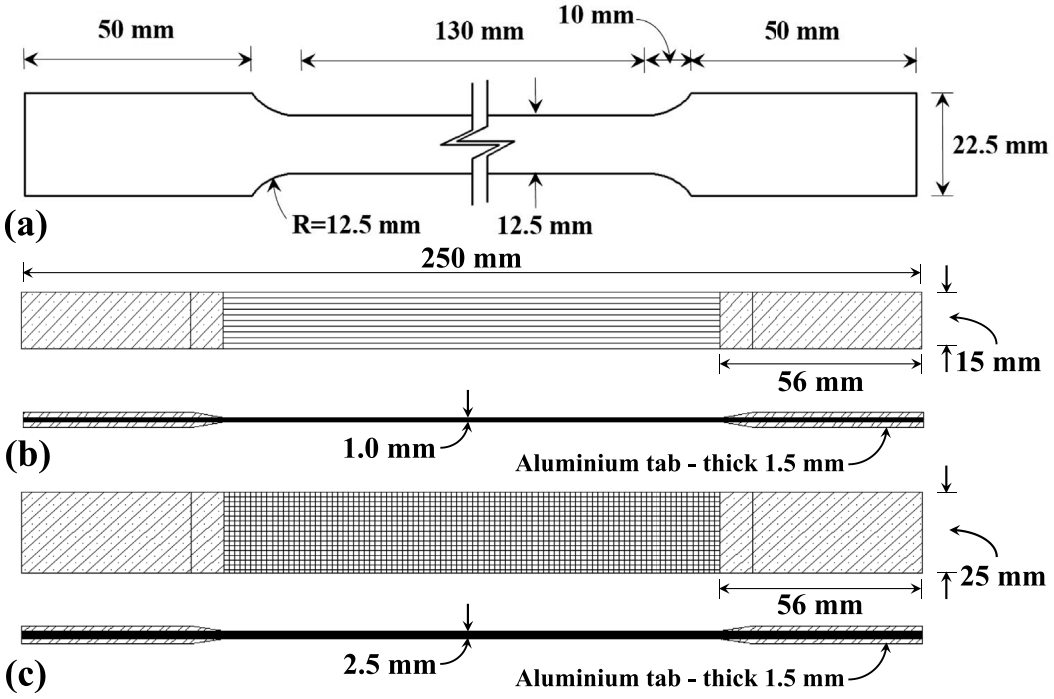

Fig. 3. Dimensions of tensile test coupons [(a) steel, (b) CFRP-Uni and (c) CFRP-Bi respectively].

dimensions arrived from ASTM E8 [35] and ASTM D3039 [36] respectively for steel and CFRP laminates. A constant displacement rate of 1 mm/min was applied for the tensile tests of both steel and CFRP specimens. The elastic modulus of steel and CFRP fabrics (E_{STEEL} and E_{CFRP}) were obtained from the initial readings of the strain gages (HBM strain gages, K-216.00-2128 Linear Strain Gauge, 6 mm grid length with 350-ohm resistance) that were instrumented in the gage length of the tensile test specimens. The stress-strain curves of steel and CFRP fabrics obtained from the tensile tests are shown in Fig. 4a and b respectively. It should be noted that the stress-strain curves of the CFRP fabrics exhibit multilinear slopes or transition points. The obtained material properties Young's modulus (E), yield stress (σ_y), strain in percentage at fracture (ε_f) and ultimate stress of CFRP fabrics from the tensile tests are summarized in Fig. 4c.

It should be noted that both the unidirectional (curves with legends "UD" in Fig. 4b) and bidirectional (curves with legends "BD" in Fig. 4b) CFRP's exhibit a transition point (marked with "+" symbol) after which there is a change in the slope (lesser than initial modulus) of the stress strain curves. This occurrence of multi linear/bi-linear response in the stress strain curve may be due to the separation of some carbon fibres from the resin matrix [1] which resulted in a loss in stiffness after reaching the stress magnitude of 552 MPa (approx.) and 250 MPa (approx.) respectively for unidirectional and bidirectional CFRP. Such fiber behavior may be attributed to the fact that the carbon fiber fabric (dry fiber sheet) employed has less GSM (grams per square inch - less fibres density) than the fibres typically used by other researchers. Therefore, it is evident that the stress-strain curve has a bilinear response. The transition strain point (significant change in slope) in the stress strain curve is determined by fitting an intersection point for the two linear regions in the stress strain curve (section >3.2.4 of [36].

The burnoff test was carried out to determine the fiber fraction ratio of the CFRP materials as per ASTM D3171-15 [37]. The fiber fraction ratio is 48% and 43% for of the unidirectional CFRP and bidirectional CFRP respectively, which satisfies the fiber volume requirement of ACI [13]. Such low fiber fraction ratio may be attributed to the low unit weight of the fabrics used; the unit weight of the unidirectional and bidirectional fabric is 230 gsm (0.3 mm thick fabric) and 200 gsm (0.2 mm thick fabric) respectively.

2.3. Specimen fabrication

The performance of the bonded CFRP to the structural member depends predominantly on the preparation of a substrate surface which is a steel surface in this study. The steel surface was wiped using solvent and roughened by using high strength steel wire brushes to remove rust and other foreign particles that may prevent proper bonding. Followed by the roughening, dry wiping was done to remove the dust. Before the commencement of wrapping work, all the required CFRP fabric layers were cut to required dimensions to avoid delay during the resin application. The mixed resin [EPOFINE-556 (Fine Finish Organics, Navi Mumbai, India), epoxy content 5.30–5.45 Equivalent/kg, density 25 °C, 1.15–1.20 g/cc] and hardener (FINEHARD- 951, Fine Finish Organics, Navi Mumbai, India) were mixed in 10:1 proportion (weigh batching) for all specimens. An epoxy content of 800 g and hardener of 80 g were used per one square meter of both uni and bidirectional CFRP fabrics for the first layer. For the successive layers of CFRP wrapping, 500 g of epoxy and 50 g of hardener were used per square meter. The difference in the usage of the amount of resin between the subsequent layers of wrapping is due to the need to saturate both the surfaces of the substrate and CFRP fabric for the first wrap; however, the second and subsequent layers were intended to

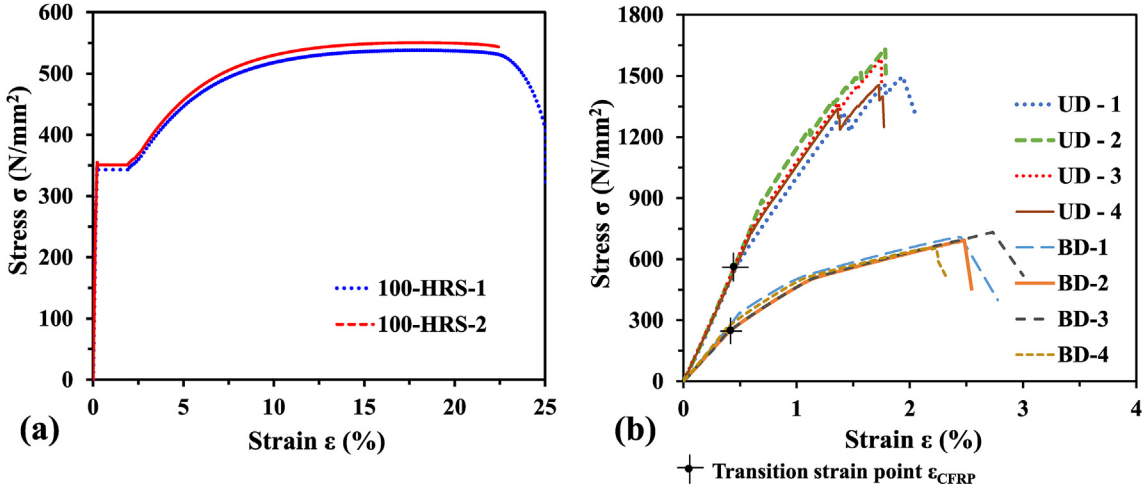

Material	E (GPa)	σ_y (MPa)	ε_f (%)
Steel Fig. 4 (a)	200	346	18

(c)

Material	E_1 (GPa)	E_2 (GPa)	σ_u (MPa)	ε_{CFRP} @ Rupture	ε_f (%)
CFRP – UD Fig. 4 (b)	123.4	76.1	1543.3	0.0180	1.94
CFRP – BD Fig. 4 (b)	66.6	26.4	698.2	0.0246	2.67

Fig. 4. (a&b) Stress-strain curves obtained from tensile tests (steel and CFRP (Uni directional and Bidirectional)); (c) Mechanical properties of steel and CFRPs.

saturate only the CFRP fabric.

ACI [13] suggests not to use the mixed resin that exceeds its specified thermosetting life since the viscosity will continue to increase from the time of mixing due to which the applied resin will not saturate the CFRP fabrics and results in inadequate adhesion between the steel surface and the CFRP fabric [13]. Therefore, the resin was mixed separately for each layer of CFRP wrapping to avoid improper wetting of CFRP fabric. Every CFRP layer is rolled prior to the next wrap for uniformity in thickness and for removal of excess resin. Also, the subsequent layers of CFRP fabrics were wrapped without any further delay to ensure that the resin in the previous layer and the resin applied to the next layer will mix and mingle together to act as one entity. As mentioned in the introduction section, the CFRP strengthening schemes were divided into three and four configurations in the tension flange strengthening scheme and U-wrap strengthening scheme respectively. The description of the CFRP layers in each wrapping scheme is given in Table 1. In each CFRP wrapping configuration, two specimens were tested to ensure the consistency of experimental results.

2.4. Test set-up

The experimental test setup for the four-point bending is shown in Fig. 5a. The length of the span between the simply supported ends is 2300 mm, and an overhang of 100 mm was provided at each support. The distance between the loading points is 800 mm as shown in Fig. 5a. The load was applied through the center of gravity of the steel beam [steel plate with C channel (Fig. 5b–i)]. The test was conducted under displacement control mode at the rate of 0.01 mm/s for all the tested specimens. The supports are semi-circular type as shown in Fig. 5a; it allows only out-of-plane rotations but not the lateral movement. To verify if the experimental support conditions simulate simple supports, the curvature obtained from the experiments were compared with the theoretical curvature. The comparison result is presented in section 4.3 "calculation approaches and results" of this manuscript. The vertical deflection at the midspan was measured using a linear variable displacement transducer. Out of the two specimens in each set of CFRP wrapping configuration, one specimen was instrumented with strain gages to measure the bending strain experienced by the

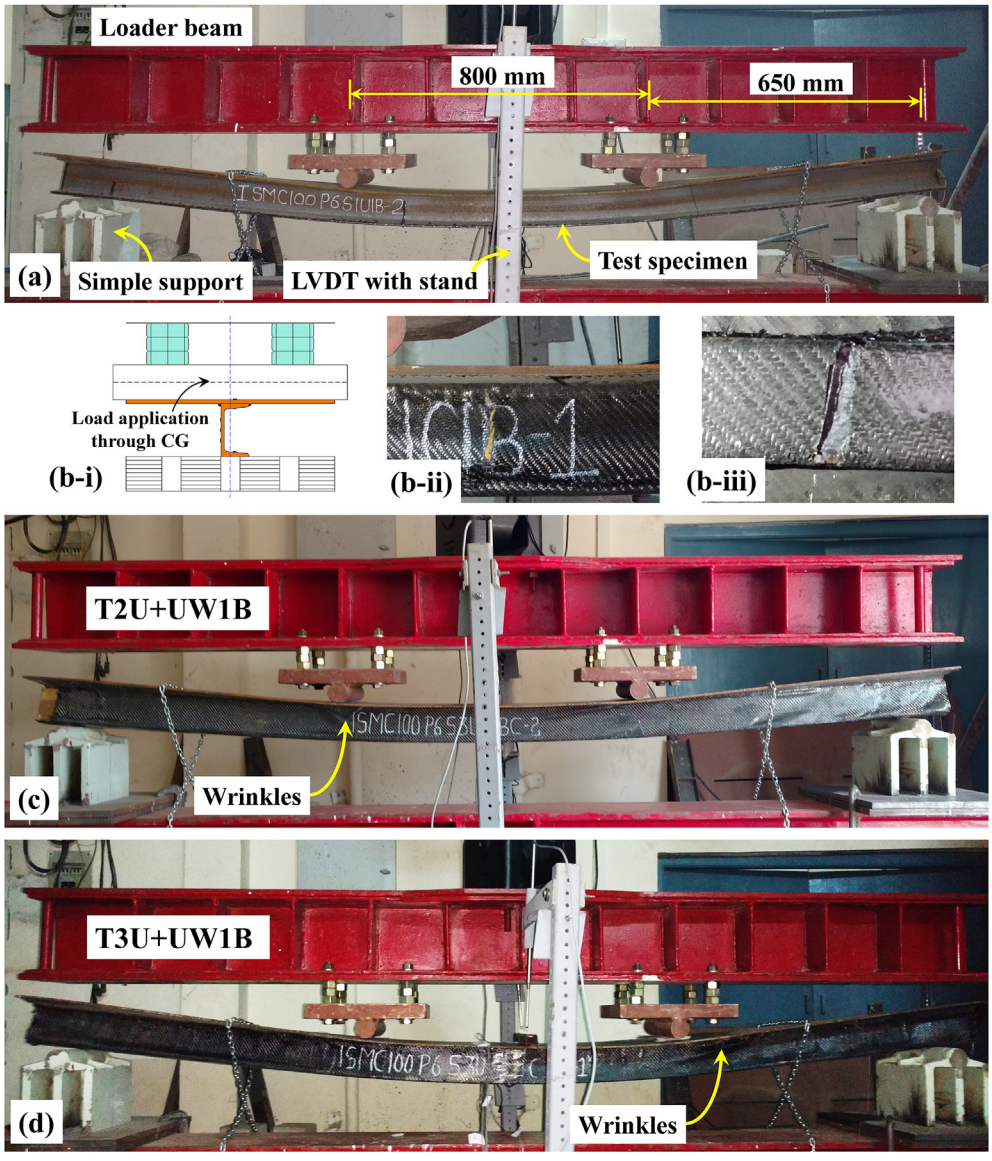

Fig. 5. (a) Experimental test setup; (b) Rupture of CFRP in T1U + UW1B specimen; (c) Occurrence of wrinkles in T2U + UW1B; (d) Occurrence of wrinkles in T3U + UW1B.

test specimen during loading. The strain gages were located such that the required bending strain profile can be captured. The location of the strain gages in the tension flange strengthening scheme and U-wrap strengthening scheme is shown in Fig. 2b and c respectively.

3. Results and discussion

3.1. General

In general, it was observed that the failure of the CFRP strengthened steel beams was either due to the debonding between the steel and CFRP or rupture of the CFRP. The different wrapping schemes and the number of CFRP layers have uniquely contributed to the strength and structural behavior of each member. However, the specimens that have the bidirectional fabric as final layer failed at lesser load than the one that has the unidirectional fabric as a final layer due to its low modulus compared to the unidirectional fabric. The ultimate load and strength improvement of each CFRP strengthening scheme with respect to the control specimen is summarized in Table 1. Overall, the CFRP strengthening scheme has improved the strength of the steel beam by 45% compared to the bare steel specimen in terms of ultimate strength. Also, it was observed that the strength improvement in the tension flange strengthening scheme was insignificant (max. of 6.7%).

3.2. Control specimen and tension flange strengthened specimens

As noted in the work description section, one bare steel beam specimen (control specimen) was tested before the CFRP strengthened specimens to quantify the strength improvement with respect to each strengthening scheme. The ultimate load of the control specimen was 20.7 kN-m, and the failure occurred due to yielding of the cross section ($M_y = S_f F_y = 16.27$ kN-m). Out of the three tension flange strengthening scheme specimen sets, two of them have a bidirectional fabric as a final layer (T1U1B and T2U1B), and the other has a unidirectional fabric as the final layer (T1U). It was observed that the specimens T1U and T2U1B were having similar flexural strength improvement (6.5% and 6.7%) compared to the control specimen even though their number of bonded CFRP layers are different. This may be attributed to the occurrence of debonding in the tension flange of specimen T2U1B due to the lower modulus of bidirectional CFRP polymer thus resulting in similar strength to the specimen that has only one unidirectional CFRP layer (T1U). It should also be noted that the average ultimate load of specimens T1U1B (20.95 kN-m) is very close to the ultimate load of the control specimen (20.72 kN-m) which indicates that the low modulus ($<E_{Steel}$) CFRP fabrics are incapable of contributing to the flexural strength improvement when they are used in the tension flange alone. However, an attempt has been made to achieve an effective strengthening scheme for steel beams using the low modulus CFRP fabrics.

3.3. U-wrap strengthened specimens

The U wrap strengthening scheme was introduced since the low modulus CFRP fabric did not contribute to the strength of the member by the tension flange strengthening scheme due to the debonding failure of uni-directional and bi-directional CFRP polymers. Since the bidirectional fabric in tension flange strengthened specimens experienced debond at the extreme tension fiber due to its low modulus, the CFRP polymers should also be installed to the portion of the webs of steel beam where the strain value is expected to be low compared to the extreme tension flanges. This is to ensure that the CFRP in the web portion can also contribute to the strength before debonding of bidirectional CFRP in the tension flange leading to the wrapping of the same low modulus CFRP's throughout the entire depth of the web portion as shown in Fig. 2c.

Four different wrapping configurations in the U-wrap strengthening scheme by altering the number and sequence of CFRP layers were considered (Table 1). The specimen that has one unidirectional fabric in the tension flange and one U wrap using the bidirectional fabric (T1U + UW1B) was found to be ineffective for flexural strengthening as it does not contribute to the strength of the member and failed in rupture as shown in Fig. 5b–ii and 5b-iii. Such rupture failure of bidirectional fabric is due to its low modulus and insufficient CFRP strengthening layers in the tension flange. It should be noted that the failure strain of the CFRP's used is higher than the yield strain of steel beam as shown in Fig. 4b. Therefore, there is a possibility that the strengthened steel beam (parent material) may have yielded in this specimen (T1U + UW1B) since the CFRP has failed in rupture. Such unconservative test results (plastification in the steel beam) needs to be taken into consideration while calculating the design strength of the beam by arriving at a design limit state that ensures the design stresses are within the elastic limit.

In the next two U-wrapping types, only the number of tension flange unidirectional wrapping was increased from single layer to double (T2U + UW1B) and triple (T3U + UW1B) layers with a final U-wrap using bidirectional fabric. The T2U + UW1B and T3U + UW1B CFRP wrapping schemes have increased the strength of the steel beam by 29.3% and 26.1% respectively compared to the control specimen. It should be noted that the strength of the T2U + UW1B and T3U + UW1B are almost same even though there is an additional unidirectional layer in the tension flange since the failure of the specimens were governed by the presence of a final bidirectional layer of wrap for both the specimens that failed due to rupture. It can be observed from Fig. 6b (T2U + UW1B) and 6c (T3U + UW1B) that the strain readings at the cardboard side did not increase gradually from the beginning of the load application to the ultimate load (deviated from the linear strain profile), due to the occurrence of wrinkles in the CFRP U-wrap (Fig. 5c and d) which has prevented the CFRP bidirectional fabric from gaining strain. This indicates that the thickness of the CFRP wrap in the web portion was not sufficient to restrain the wrinkling in the shear span of the beam. Nevertheless, the improvement in strength in U-wrap specimens (T2U + UW1B and T3U + UW1B) is significantly higher than the tension flange strengthening schemes, and this may be attributed to the contribution from the fibers present on both sides of the web portion. Though the strength of the steel beams was improved, the occurrence of wrinkles in the U wrap is not a reliable failure mode. Such failure modes should be avoided either by increasing the thickness of the wrap or by limiting the design strain in the design calculations.

To overcome the wrinkle effect, the thickness of the U-CFRP wrap was increased by increasing the CFRP layer from one (0.2 mm) to two (0.4 mm). After adding an additional U-wrap the specimen with three layers of unidirectional CFRP layers in the tension flange and two layers of U-wrap using bidirectional CFRP (T3U + UW2B) improved the strength (mean value 30.17 kN-m) of the member by 12.6%, 15.5% and 45.6% compared to the specimen configurations T2U + UW1B, T3U + UW1B and control specimen respectively. It can be observed from Fig. 6d that the strain reading on the steel side as well as the cardboard side for specimen configuration T3U + UW2B increased steadily from the initial application of the load to the ultimate load (linear strain profile). This gradual increase in strain value indicates an absence of wrinkling effect followed by an increase in flexural capacity due to the increased thickness of the CFRP wrap from one layer (0.2 mm) to two layers (0.4 mm). It indicates that the low modulus CFRP can also be used effectively for the flexural strengthening of the steel structures provided an adequate number of CFRP layers installed in optimized

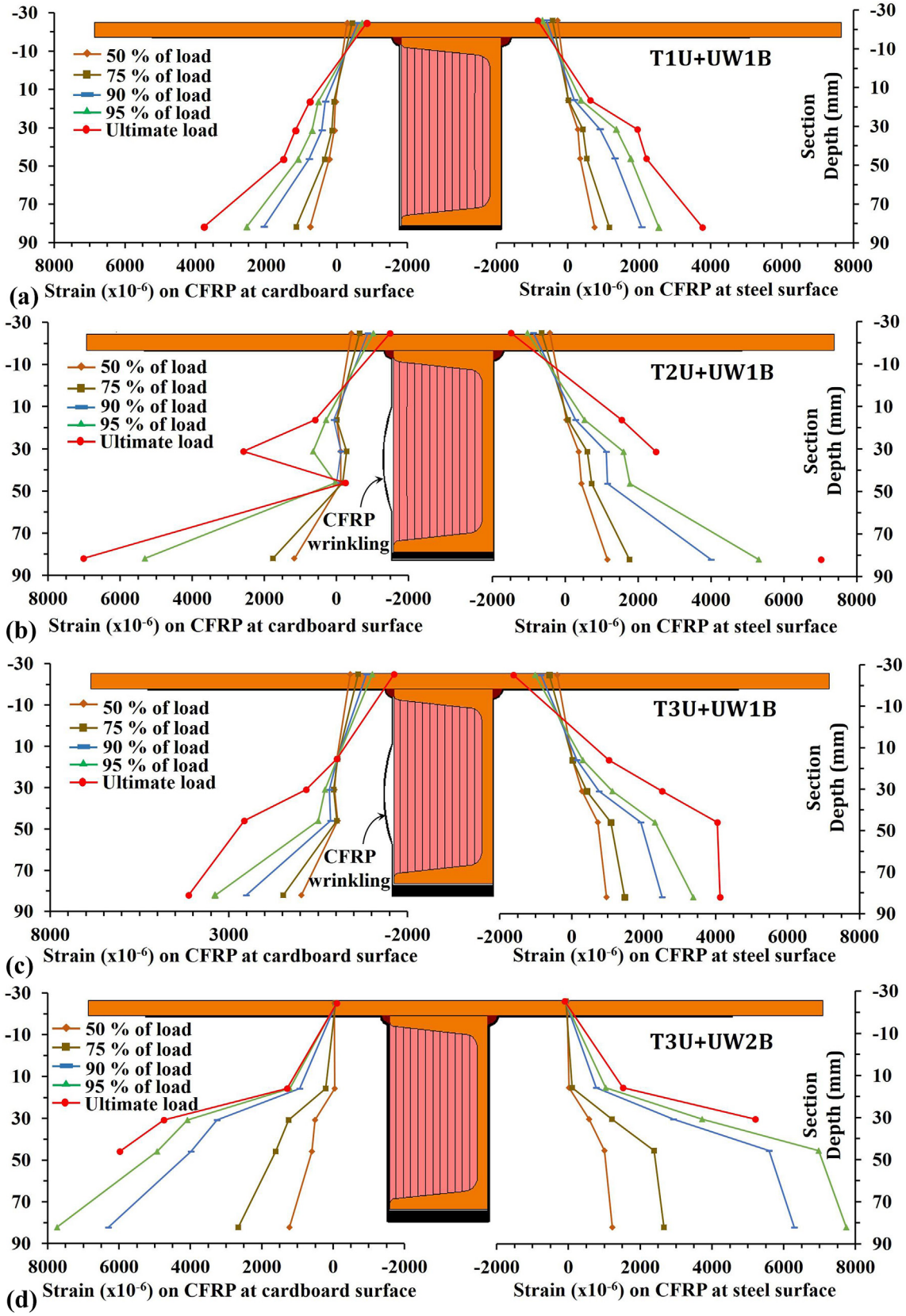

Fig. 6. Strain profile obtained from the experiments: (a) T1U + UW1B specimen; (b) T2U + UW1B specimen; (c) T3U + UW1B specimen; (d) T3U + UW2B specimen.

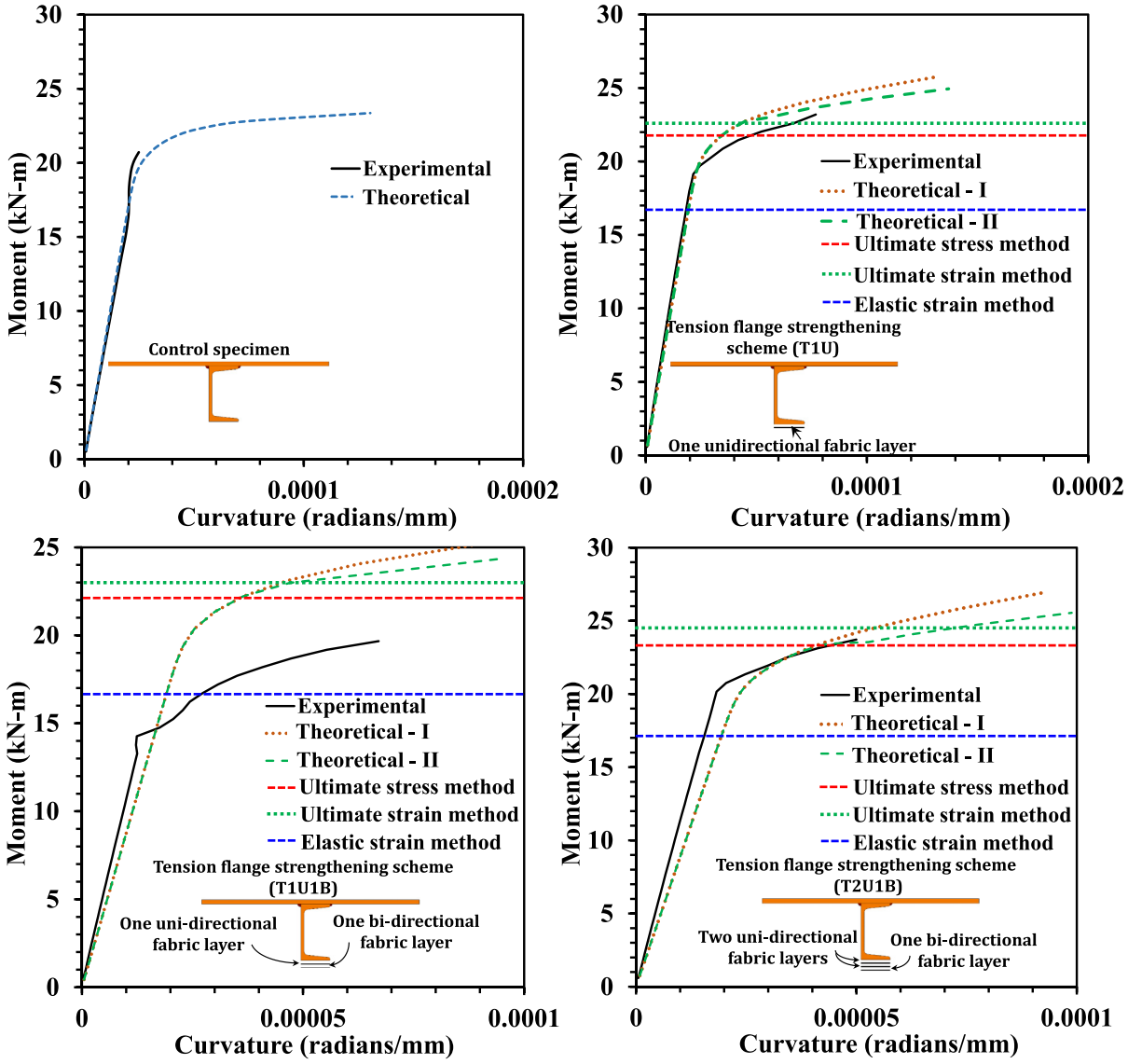

Fig. 7. Experimental versus theoretical results comparison: (a) Control specimen; (b) T1U specimen; (c) T1U1B specimen; (d) T2U1B specimen.

wrapping configurations are employed.

4. Theoretical model and design - comparison

4.1. CFRP strengthened composite beam design

In the CFRP strengthening schemes for structural steel beams using the low modulus CFRP fabrics, the governing mode of failure was either due to rupture or debonding of the CFRP in the tension flange. However, to ensure that the CFRP strengthened structural steel beam remains within the elastic limit under the service load, the values of stress and strain in the extreme tension fiber of the CFRP wrapped member should be under the elastic limit. In addition, the design strain magnitudes should also be limited to prevent any undesirable failure modes such as debonding or CFRP rupture [1,4]; and [13].

The CFRP fibers used in the present study have low modulus with a stress-strain curve that has multi-linear behavior with different moduli separated by a transition strain point as shown in Fig. 4b. Therefore, it is important to determine the appropriate material model of the CFRP before employing the same for design calculations. In the present work, three different design philosophies have been used as per the current design provisions [1,4,5,9–13] and [14]. However, the design philosophies were incorporated after identifying the correct calculation method that includes material nonlinearity.

4.2. Calculation approaches and results

Two different calculation approaches have been attempted in this work.

a) The Theoretical-I approach assumes a linear behavior of the CFRP, where the value of E_{CFRP} is constant until the ultimate design stress is reached.
b) The Theoretical-II approach follows a multi-linear behavior of the CFRP where the value of E_{CFRP} was used based on the varying stress-strain curve as shown in Fig. 4b.

The moment-curvature relationships obtained from both the calculation approaches for all the tested specimens were compared with the experimental moment-curvature relationship in Figs. 7

and 8. It should be noted that in Figs. 7c and 8a, the Theoretical I and II approach results are higher than the experimental results for the specimens T1U1B and T1U + UW1B. This may be attributed to the cross section twist of the specimens T1U1B and T1U + UW1B during loading thereby leading to a significant loss of vertical bending stiffness. Except for the two specimens (T1U1B and T1U + UW1B), the theoretical moment-curvature curves closely matched with the curves from the experimental moment-curvature. This indicates that the experimental support conditions are simulating the simple supports. Besides, the comparison indicates that the Theoretical II (following the multi-linear stress-strain curve) approach has a higher correlation to the experimental moment-curvature than the Theoretical I (using the linear stress-strain curve) approach. This is because of the fact that the Theoretical II approach considers both the modulus values [E1 and E2 (Fig. 4c)] from the stress-strain curve of the CFRP fabrics obtained from the tensile test (Fig. 4b). This verification between the Theoretical I and II approaches is required since the available design methods [27,28] are only for the high modulus CFRP's with a single modulus value until failure (linear stress-strain curve).

4.3. Design philosophies

The suggested general provisions for the design of CFRP strengthened beam is the maximum design stress (max. F_{CFRP}) or design strain (max. ε_{CFRP}) to be considered according to Eqs. (2) and (3) given in ACI [13].

$$F^{*}_{CFRP} = C_E(F_{CFRP} - 3\sigma) \tag{2}$$

$$\varepsilon^{*}_{CFRP} = C_E(\varepsilon_{CFRP} - 3\sigma) \tag{3}$$

where $F_{CFRP}{}^{*}$ and $\varepsilon_{CFRP}{}^{*}$ are the maximum design stress and strain of the CFRP to be used in the design; F_{CFRP} and ε_{CFRP} are the mean ultimate stress and strain of the tensile tests conducted (Fig. 4c); σ is the standard deviation of the ultimate stress and strain obtained from the tensile tests; C_E is the environmental reduction factor (C_E) as per Table 9.4 of ACI [13].

Equations (2) and (3) account for both the standard deviation (σ) of the obtained stress from the tensile test as well as the environmental reduction factor (C_E) to consider the possible degradation of the composite materials in the exterior environment as per

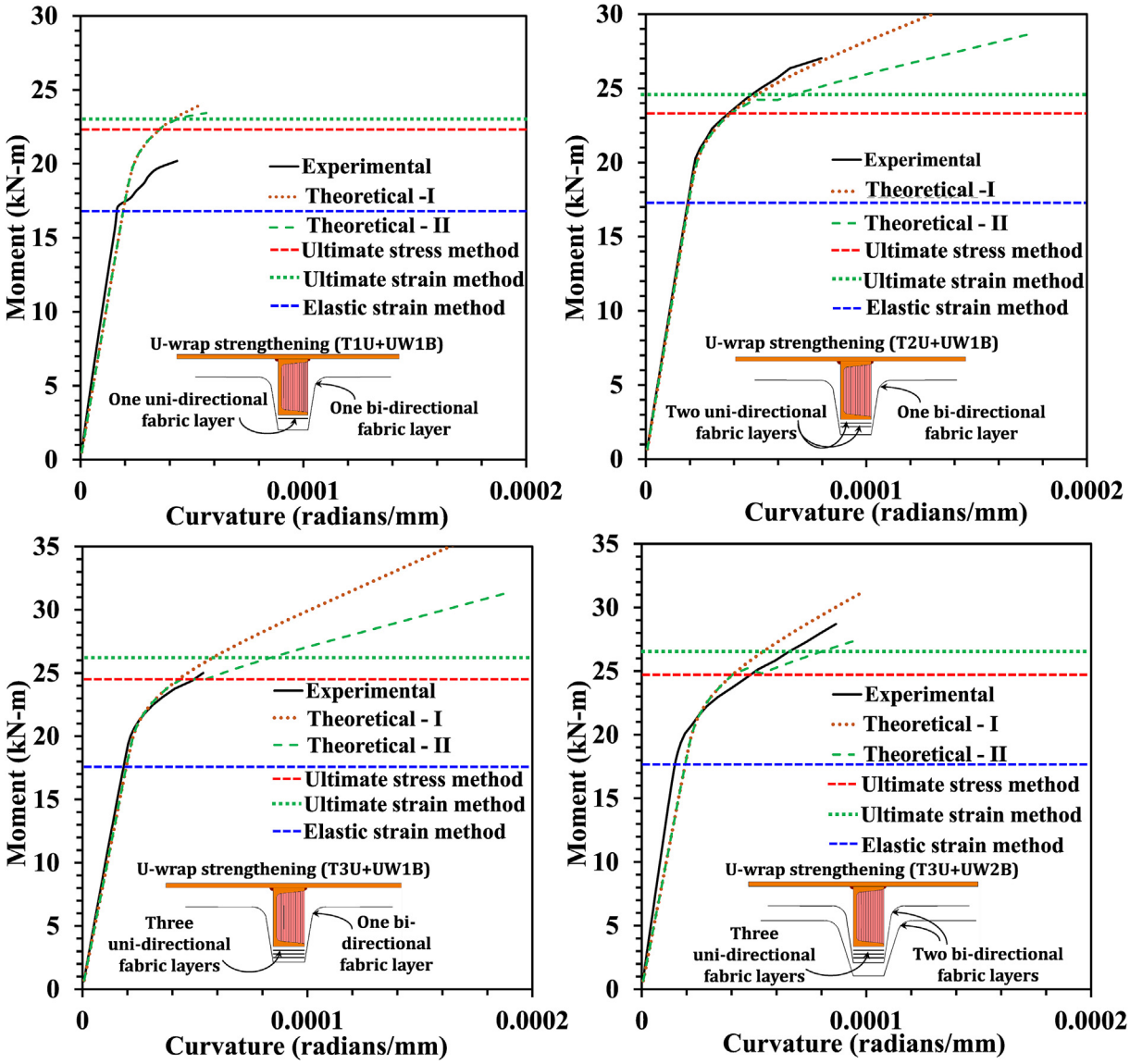

Fig. 8. Experimental versus theoretical results comparison: (a) T1U + UW1B specimen; (b) T2U + UW1B specimen; (c) T3U + UW1B specimen; (d) T3U + UW2B specimen.

Table 9.4 of ACI [13]. It should be noted that the ACI [13] specifies different environmental reduction factors for interior and exterior environments. In the current design stress and design strain calculations, an environmental reduction factor of 0.85 (per Table 9.4 of ACI [13] for CFRP was considered by assuming the exposure conditions exterior or aggressive for conservativeness.

4.3.1. Design philosophies: various design methods

When the high-modulus ($E_{CFRP} > E_{STEEL}$) CFRP's are used for flexural strengthening of steel members, either the ultimate stress or the ultimate strain of the CFRP's can be used as a design limit state, since the high-modulus CFRP's typically exhibit a single linear stress-strain relationship where the design stress or design strain leads to the same design prediction. This indirectly means that the rupture of fibers will occur first in the high-modulus CFRP before yielding occurs in the steel substrate [ε_S at yield > ε_{CFRP} of high-modulus CFRP at rupture (Fig. 9a)] as shown in Fig. 9c. In the case of low modulus FRP ($E_{CFRP} < E_{STEEL}$) strengthening schemes (present study), the steel substrate will yield before the debonding or rupture of CFRP as shown in Fig. 9d if the ultimate stress, or strain of the FRP material was used as a design limit state as per current design provisions [1,4,5,9–13] and [14], since the yield (ε_S at yield) strain of the steel is less than the CFRP (ε_{CFRP} at rupture) (Fig. 9a). Hence, the limit state of ultimate stress of CFRP as a design criterion for the design of steel beams strengthened with low modulus CFRP will result in unconservative predictions due to the debonding between the steel and CFRP. Therefore, it is necessary to check the design capacity of the strengthened steel beam either up to the elastic strain limit of steel or ultimate strain limit of CFRP whichever is conservative limit state for the design of structural members strengthened with low modulus CFRP. Therefore, three different design limit states (ultimate stress method, ultimate strain method, and elastic method) were evaluated for the present design work to identify the limit state that leads to conservative results. All the

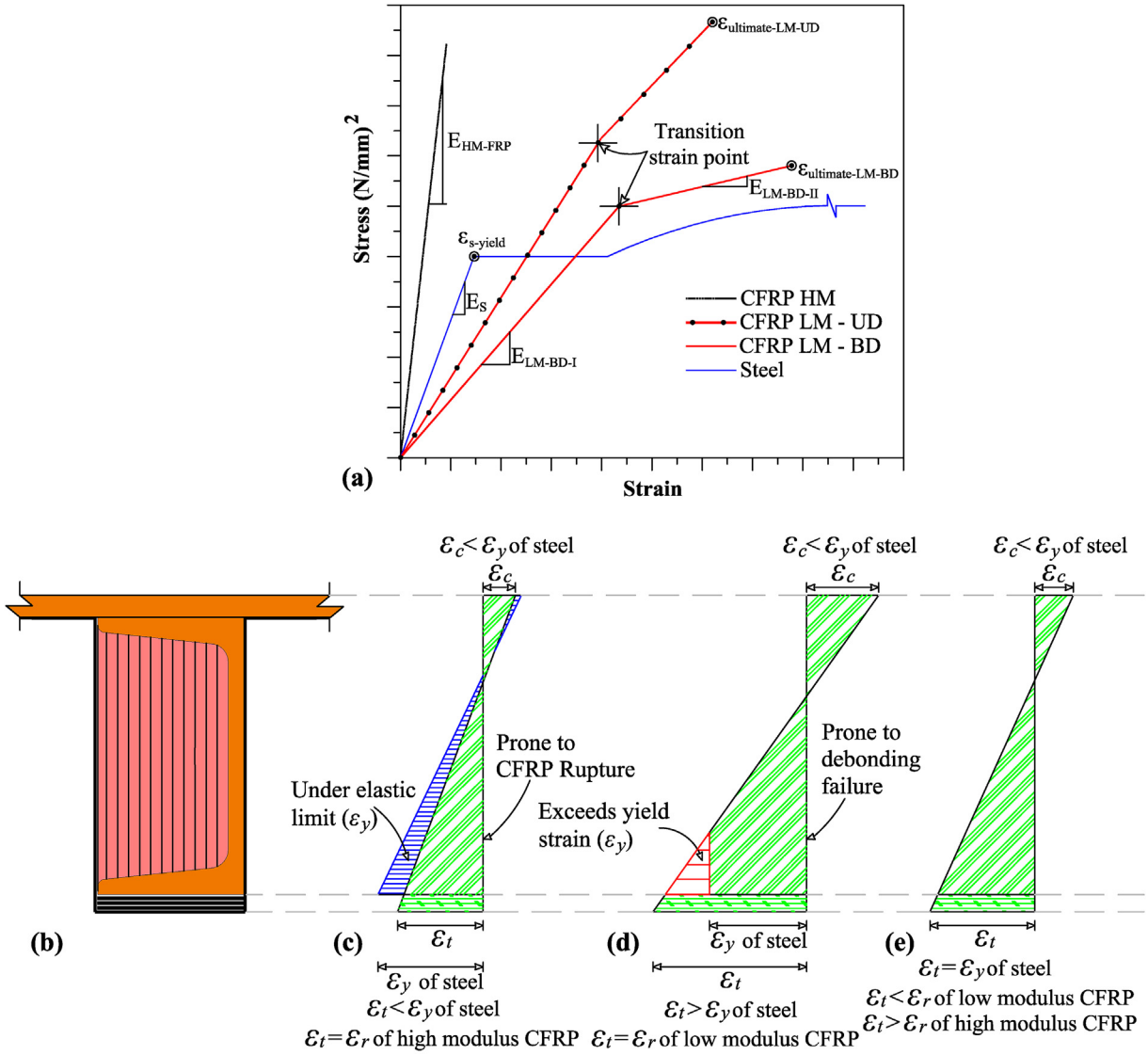

Fig. 9. a). Stress-strain plot for the steel, high modulus CFRP and low modulus CFRP; Design limit states: b). C/s view of the composite beam (Steel and CFRP); c). Bending strain profile for the design limit state of ultimate stress or ultimate strain (high modulus FRP); d). Bending strain profile for the design limit state of ultimate stress or ultimate strain (low modulus CFRP); e). Bending strain profile for the design limit state of elastic strain (low modulus CFRP).

three different design calculations were carried out using the Theoretical II approach which follows the multi-linear stress-strain curve of CFRP.

1. Ultimate stress method ($M_{d\ (CS\text{-}\sigma u)}$): The maximum design stress of FRP fabrics or sheets that can be considered for the design calculations is given in Eq. (2) [13]. Therefore, the ultimate stress calculated for the unidirectional and bidirectional fabrics will be used for the beam designs respectively for the specimens that have the unidirectional fabric (T1U) and bidirectional fabric (T1U1B, T2U1B, T1U + UW1B, T2U + UW1B, T3U + UW1B, and T3U + UW2B) as a final strengthening layer. After finding the ultimate design stress using Eq. (2) it is difficult to find the corresponding strain in case of CFRP fabrics that is having multilinear stress-strain curves (Fig. 9a). This is because the manufacturer typically does not provide the tangent modulus and or the subsequent modulus values and provide only a single Young's modulus (*E*-initial), ultimate tensile stress (σ_u) and percentage elongation values. Therefore, the corresponding strain value calculated by dividing the ultimate stress (σ_u) of the CFRP with the initial Young's modulus (E_{CFRP}) may lead to erroneous estimation of ultimate strain. This indicates that the use of new material (low modulus CFRP with multilinear stress-strain curves) requires a change in the design limit state rather than questioning the applicability of using current Ultimate stress method. However, the calculations are presented as a confirmation to prevent the use of this approach for design purposes.

2. Ultimate strain method ($M_{d\ (CS\text{-}\varepsilon u)}$): The maximum strain to be considered in the design can be determined from Eq. (3) for both the unidirectional and bidirectional fabrics. It should be noted that two different modulus CFRP fabrics were used in this design work which is also bonded together as one over another (*ex.* T1U1B and T1U + UW1B). In that case, if the highest strain value (ultimate strain value of the low modulus fabric) among the two (unidirectional and bidirectional) is used to arrive at design stress, then there is a possibility that the fabric having low ultimate strain may fail before the higher strain fabric. To avoid such a phenomenon, the lowest strain value should be used as a design strain irrespective of the modulus value. Therefore, in the present study, the ultimate strain of the unidirectional fabrics ($\varepsilon_{CFRP\text{-}U}$) was used as the design strain in design strength calculations since the ultimate strain of the bidirectional fabric ($\varepsilon_{ultimate\text{-}LM\text{-}BD}$) was higher (see Figs. 4b and 9a). However, this method will lead to plastification of the structural steel member as shown in Fig. 9d since the ultimate strain of the CFRPs ($\varepsilon_{ultimate\text{-}LM\text{-}UD}$ and $\varepsilon_{ultimate\text{-}LM\text{-}BD}$) used in this work is higher than the structural steel ($\varepsilon_{s\text{-}yield}$) (see Fig. 9a).

3. Elastic strain method ($M_{d\ (CS\text{-}\varepsilon E)}$): It should be noted that the steel beam has the highest elastic modulus (E_S) among all the other materials in the present composite member design work as shown in Fig. 9a. Therefore, to ensure that the entire cross section remains within the elastic limit, the maximum elastic strain of the structural steel should be used as a design strain since this will have lowest strain limit before any occurrence of yielding or debonding (between steel and CFRP) in the cross-section (Fig. 9e). Hence, the elastic strain of the steel (ε_{steel} at yield) obtained from the stress-strain curve of the steel material as shown in Fig. 4a was used in the design calculations. Therefore, the following Eq. (4) or (5) can be used as an alternative approach to obtain the design strain for the elastic strain method ($M_{d\ (CS\text{-}\varepsilon E)}$) when the steel members subjected to flexure are strengthened with low-modulus CFRP. However, this method will not be suitable for the flexural member strengthened with high modulus ($E_{CFRP} > E$ of strengthened parent material) CFRP materials.

$$\varepsilon_{CFRP(d)} = C_E(\varepsilon_{CFRP} - 3\sigma) \text{if } E_{CFRP} > E_{STEEL} \tag{4}$$

$$\varepsilon_{s.elastic} = \frac{f_y}{E_s} \text{ if } E_{CFRP} < E_{STEEL} \tag{5}$$

where $\varepsilon_{CFRP(d)}$ and $\varepsilon_{s.elastic}$ are the maximum design strain values to be used in the design respectively for CFRP and steel; f_y and E_s are the yield stress and Young's modulus of the steel obtained from the tensile test (Fig. 4c). The design procedure involved in this manuscript is explained in the following section.

4.4. Calculation procedure

The design of a strengthened steel beam using low modulus CFRP was carried out using the moment-curvature relationship. In the design strength calculation procedure, both the composite cross section (Fig. 10) and the nonlinear properties of the materials (Fig. 4) were considered. The moment-curvature relationship curve of the test specimens was obtained by incrementally increasing the strain at the extreme tension flange of the CFRP fabric (unidirectional or bidirectional).

The entire depth of the specimen cross section was divided into

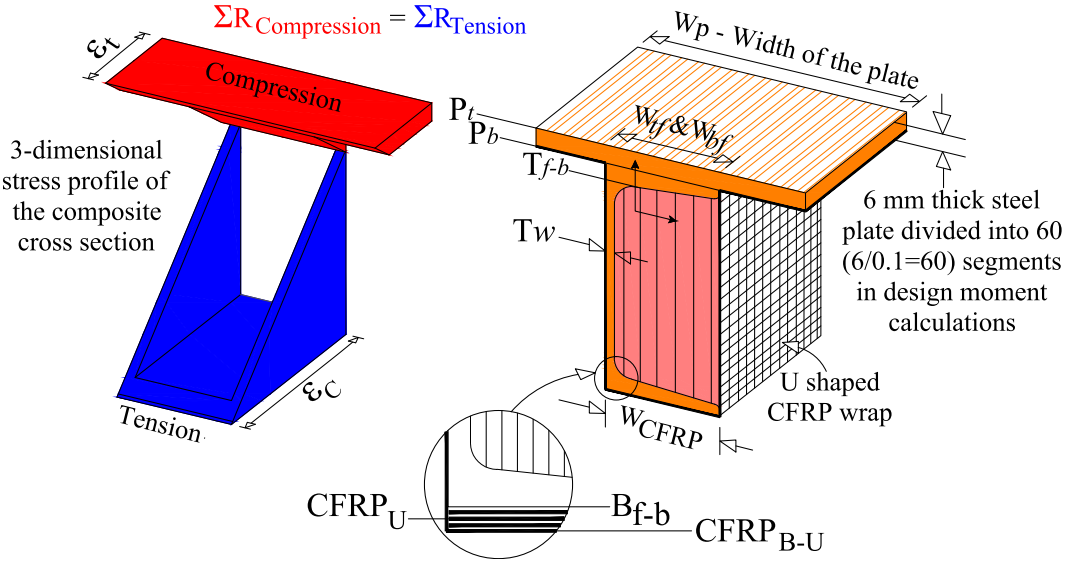

Fig. 10. Three dimensional strain profile of the composite section and the details of the segments divided for calculation of moment-curvature.

Table 3
Comparison between the design methods.

Specimen	$M_{EXP}/M_{d\ (S)}$ (IS 800)	Theoretical II Approach		
		M_{EXP}/M_d (CS- σU)	M_{EXP}/M_d (CS- εU)	M_{EXP}/M_d (CS- εE)
T1U	1.44	1.01	0.97	1.32
T1U1B	1.37	0.95	0.91	1.25
T2U1B	1.45	0.95	0.90	1.29
T1U + U1B	1.34	0.92	0.89	1.22
T2U + U1B	1.75	1.15	1.09	1.56
T3U + U1B	1.71	1.07	1.00	1.49
T3U + U2B	1.97	1.23	1.14	1.70
Mean		1.04	0.99	1.40
St.dev (σ)		0.116	0.098	0.181
Reliability Index (β)		2.91	2.76	3.89

segments for better accuracy as shown in Fig. 10. The force equilibrium (the force above the neutral axis and below the neutral axis to be equal) was maintained throughout the calculation of curvatures (ϕ) and the corresponding moment values. The force equilibrium for each increment in tension flange strain (ε_{CFRP}) was achieved by iterating the neutral axis location. After achieving the force equilibrium, the curvature (ϕ) and the corresponding moment was determined from Eqs. (6) and (7) respectively.

$$\phi = \frac{\varepsilon}{d_n} \tag{6}$$

where ϕ is the curvature; ε and d_n are the strain and depth of neutral axis from the extreme tension fiber respectively. The moment capacity for each increment in strain was calculated by the sum of multiplication of all the resultant forces (R) of each segment and their corresponding distance ($\overline{X}$) from the neutral axis, as shown in Eq. (7),

$$M = \sum R\overline{\overline{X}} \tag{7}$$

The force equilibrium of the section for each strain increment was determined by adding the resultants of each segment, as shown in Eq. (8),

$$\sum R = 0 \tag{8}$$

The resultant force (R) of each segment of the design cross section was determined by multiplying the stress (F_s) and the area (segment depth * segment width) of the respective segments. The calculation of resultant force for each segment in the design cross section was calculated using Eq. (9).

$$R = \int_a^b F(x)b(x)dx \tag{9}$$

The stress at each increment of strain was calculated by Eqs. (10) and (11) for steel and CFRP respectively. Equation (6) is the modified Ramberg-Osgood function, recommended by Mattock [38] used in this present study to incorporate the nonlinear stress-strain curve of structural steel and Eq. (7) is a direct multiplication of Young's modulus (E_{CFRP}) of the CFRP to the corresponding strain (ε_{CFRP}).

$$F_s(x) = E_s\varepsilon_{s(x)}\left[A + \frac{1-A}{\left[1+(B\varepsilon_{s(x)})^C\right]^{\frac{1}{C}}}\right] \tag{10}$$

$$F_{CFRP}(x) = E_{CFRP}\varepsilon_{CFRP(x)} \tag{11}$$

where F_s (x) is the stress in the steel; E_s is Young's modulus of the steel from the tensile test; $\varepsilon_{s(x)}$ is the strain at the corresponding segment of the steel section; A, B and C are the Ramberg-Osgood parameters that can be determined from the stress-strain curves of the steel specimens; the determined values of A and B are 0,

Table 4
A design example for predicting the design strength of the steel flexural member strengthened using low modulus CFRP.

Design Steps	Ultimate stress method	Ultimate strain method	Elastic strain method
Assuming Strain at the bottom flange (ε)	FCFRP* = CEFCFRP-3σ F_{CFRP} * = 0.85(1542.98 −3(82)) F_{CFRP} * = 1102.4 N/mm^2 $\varepsilon = \sigma E$ = 1102.4123400 ε = 0.008934	εCFRP* = CEεCFRP-3σ ε_{CFRP}* = 0.85(0.017985 −3(0.000965)) ε_{CFRP} * = 0.012827 ε = 0.012827	$\varepsilon s.elastic$ = 0.00173 Using Eq. (11).
Iteration 1			
Assuming neutral axis (d_n) (from bottom)	92 mm	92 mm	92 mm
Determination of curvature using Eq. (2).	$\phi = 9.71 \times 10^{-5}$	$\phi = 1.39 \times 10^{-4}$	$\phi = 1.88 \times 10^{-5}$
Determination of stress [F_s (x) and F_{CFRP} (x)] at the each segment of the cross section using Eqs. (6) and (7) respectively.			
Determination of resultant force (R) for each section using Eq. (5).	Total resultant force ($\sum$R) = −137251.35 N	Total resultant force ($\sum$R) = −292517.54 N	Total resultant force ($\sum$R) = 120729.17 N
Since the total resultant force (compression force + tension force) is not equal to "zero", The neutral axis depth (d_n) needs to be changed such that the total resultant force will become zero (achieving the force equilibrium).			
Iteration 2			
Assuming neutral axis (d_n) (from bottom)	94.925 mm	96.695 mm	81.661 mm
Determination of curvature using Eq. (2).	$\phi = 9.41 \times 10^{-5}$	$\phi = 1.33 \times 10^{-4}$	$\phi = 2.1185 \times 10^{-5}$
Determination of stress [F_s (x) and F_{CFRP} (x)] at the each segment of the cross section using Eqs. 12 and 13 respectively.			
Determination of resultant force (R) for each section using Eq. (5).	Total resultant force ($\sum$R) = 0 N	Total resultant force ($\sum$R) = 0 N	Total resultant force ($\sum$R) = 0 N
Since the force equilibrium is achieved ($\sum$R = 0), the next step in the design is to calculate the design moment.			
Determination of moment (M) by multiplying the resultant force [R (x)] of each segment in the cross section with the distance from the neutral axis (d_n). Eq. (3).	M = 22.15 kNm	M = 23 kNm	M = 16.77 kNm

Design Data: Calculate the design moment for the steel beam strengthened in the bottom flange with one unidirectional CFRP layer (first layer) and one bidirectional CFRP layer (second layer). The steel beam is a built-up section, made of ISMC 100 steel channel welded with a 6 mm × 300 mm steel plate on the top flange of the C channel as shown in Fig. 2b. E_s = 200 GPa; σ_y = 346 MPa; $\varepsilon s.elastic$ = 0.00173; $E_{CFRP\ (UD)}$ = 123.4 GPa; $E_{CFRP\ (BD)}$ = 66.6 GPa;

Table 5
Low modulus vs. High modulus CFRP – Flexural Strength improvement.

CFRP Type	Tensile modulus (GPa)		Thickness of CFRP Fabric (mm)		Design strain value	Wrapping configuration (only U wrap)		Design strength of the CFRP strengthened beam[e] (kNm)	Percentage improvement in strength compared to the control specimen's design strength (Eq. (1))
	Uni	Bi	Uni	Bi		Uni	Bi		
Low modulus[a]	123.4	66.6	0.3	0.2	0.00173[c]	5 layers	3 layers	20.10	31.4
Normal modulus[b]	250	250	0.3	0.2	0.0015[d]	2 layers	4 layers	19.44	27.05
High modulus[b]	550	333.3	0.3	0.2	0.0015[d]	2 layers	2 layers	20.43	33.52

[a] CFRP that exhibits bilinear stress-strain response.
[b] CFRP that exhibits linear stress-strain response until failure.
[c] Design strain value is limited to yield strain of steel.
[d] Design strain value is based on ultimate stress/strain method.
[e] Design calculation is same as demonstrated in Table 4.

578.03 respectively for the tested steel coupons (Fig. 4a). The value of A represents the stiffness after the occurrence of yielding in the steel specimen and has been assumed conservatively as zero by considering stress-strain curve of the steel as elastic-perfectly plastic (zero slope line after yielding). The value of B is the ratio between elastic stiffness and yield strength. Since the material model is assumed as zero slope after yielding with a value of A is equal to 0, the value "C" does not play a vital role [27,28].

4. Design results and discussion

The results of the design moment calculations using ultimate stress ($M_{d\ (CS\text{-}\sigma u)}$), ultimate strain ($M_{d\ (CS\text{-}\varepsilon u)}$) and elastic strain ($M_{d\ (CS\text{-}\varepsilon E)}$) methods along with a comparison among them are given in Tables 2 and 3 respectively. For ease of understanding, a design example for predicting the design strength of the steel flexural member strengthened using low modulus CFRP has been provided in Table 4. It can be observed from Tables 2 and 3 that the results of elastic strain method ($M_{d\ (CS\text{-}\varepsilon E)}$) is conservative with respect to the experimental results (M_{EXP}), whereas the design strengths obtained from the ultimate stress ($M_{d\ (CS\text{-}\sigma u)} > M_{EXP}$ for 3 specimens) and ultimate strain ($M_{d\ (CS\text{-}\varepsilon u)} > M_{EXP}$ for 4 specimens) methods are higher than the experimental results (M_{EXP}). As mentioned previously, this unconservative strength predictions by the ultimate stress ($M_{d\ (CS\text{-}\sigma u)}$) and ultimate strain ($M_{d\ (CS\text{-}\varepsilon u)}$) methods may be due to the fact that the rupture strain of CFRP is higher than the yield strain of steel, leading to the occurrence of debonding in the CFRP strengthened specimens as shown in Figs. 7 and 8. This indicates that the ultimate stress and ultimate strain method of design strength calculations are not suitable for the design of flexural members strengthened with low modulus CFRP fabrics that exhibit multilinear stress-strain response.

5. Reliability analysis

Reliability analysis was carried out to verify the suitability of the elastic strain design limit state for design applications of the steel beams. A reliability analysis according to Plevris [39]; Okeil et al. [40]; Zureick et al. [41]; Bambach et al. [42]; Wang et al. [43]; Galasso et al. [44]; Wang and Ellingwood [45]; was performed for the test results. When the calculated reliability index value (β) based on the limited test results attain or exceed the target reliability index ($\beta_o = 3.5$) value suggested by AASHTO [46] and other researchers [Okeil et al. [40]; Nowak and Szerszen [47]; Szerszen and Nowak [48]; Wang and Ellingwood [45] and ACI [13]] for members subjected to flexure, then it can be assumed that the suggested design limit state is probabilistically conservative. The calculated reliability index values given in Table 3 indicates that the β value of $M_{EXP}/M_{d\ (CS\text{-}\ \varepsilon E)}$ (elastic strain limit state design results) is higher than the target reliability index ($\beta = 3.89 > \beta_o = 3.5$). Hence it is verified that the suggested elastic strain design limit state for the steel beams strengthened with low modulus CFRP is reliable.

In addition, it should also be noted that when such low modulus CFRP's are used for strengthening applications of steel beams (without concrete composite cross-sections), the probability of occurrence of delamination is very less since the strain value does not exceed the elastic limit ($\varepsilon_{s.elastic}$) of steel. Typically, the debonding strain (0.9 times of ultimate rupture strain of CFRP) is higher than the elastic strain of steel (typically ranging from 0.0015 to 0.002) (Section 10.1 of [13]. The design comparison between low and high modulus CFRP shown in Table 5 indicates that the strength improvement due to the low modulus CFRP (31.4% - 2.1 mm thick CFRP layers) is equal to the higher modulus CFRP (27.05% - 1.5 mm thick CFRP layer and 33.52% - 1 mm thick CFRP layer). This indicates that the use of low modulus CFRP's can also be used as an acceptable means of strengthening steel sections.

6. Conclusions

An experimental and analytical investigation retrofitting of steel beams using low modulus CFRP has been presented. Unlike the existing methodologies (ultimate stress and ultimate strain design limit states) that are typically employed for design of strengthening of steel members using high modulus CFRP ($E_{CFRP} > E_{Steel}$), a conservative design limit state has been presented specifically for the use of low modulus CFRP ($E_{CFRP} < E_{Steel}$) as a potential alternative. Although, it may appear that the suggested elastic strain limit is a conservative approach, an increase in strain limit higher than the elastic strain may result in debonding between steel and CFRP. Also, in case of structural steel members strengthened using high modulus CFRP, the design strain limits will be below the elastic strain ($\varepsilon_{s,elastic}$) of steel by limiting the design strain equal to the ultimate strain of CFRP to avoid failure due to CFRP rupture. While the quantity of low modulus of CFRP required for retrofitting may be more than high modulus CFRP as demonstrated by means of a comparative design example (Table 5), the availability and affordability of low modulus CFRP poses an attractive option in comparison with high modulus CFRP.

The following specific conclusions can be drawn from the presented work:

1. The test results indicate that the strength of the flexural members can be increased up to 46% in terms of ultimate strength with respect to the control specimen.
2. A theoretical model based on the material properties and strain compatibility was used to predict the strength of the member. Three different design methods namely, maximum stress method, maximum strain method, and elastic strain method were presented for designing the flexural strength of the CFRP strengthened member.
3. The design results indicate that the predicted design strengths using ultimate stress ($M_{d\ (CS\text{-}\sigma u)}$) and ultimate strain ($M_{d\ (CS\text{-}\varepsilon u)}$) methods of ACI were relatively unconservative compared to the strength obtained from experiments.
4. The predicted design strengths using elastic strain method ($M_{d\ (CS\text{-}\varepsilon E)}$) were found to be conservative with all the experimental results.
5. It was also found that the design flexural strength of the member can be improved up to 31% with respect to the design strength of the control specimen (within the elastic strain limit) with 2.1 mm thickness of low modulus CFRP layer. Hence, a low modulus CFRP may be considered as a retrofitting strategy for structural steel members.

The present study adopted the current design provisions [1,4,10–13] and [14] (ultimate stress and ultimate strain method) for the flexural member strengthened using low modulus CFRP and found to be unconservative. Therefore, the suggested elastic limit state may be used for the design of steel members strengthened with low modulus CFRP.

Acknowledgments

The investigation reported in this paper was funded by a research grant (SB/FTP/ETA-93/2013) from the Department of Science and Technology (DST), Government of India. The authors would like to gratefully acknowledge Pennar Engineered Building Systems Ltd., Hyderabad, India, for their help in fabricating the test specimens required for experimental investigation.

References

[1] X.L. Zhao, FRP-strengthened Metallic Structures, CRC Press, Boca Raton FL USA, 2014.
[2] C. Bakis, L. Bank, V. Brown, E. Cosenza, J. Davalos, J. Lesko, A. Machida, S. Rizkalla, T. Triantafillou, Fiber-reinforced polymer composites for construction - state-of-the-art review, J. Compos. Constr. 6 (2) (2002) 73–87.
[3] A.H. Al-Saidy, F.W. Klaiber, T.J. Wipf, Repair of steel composite beams with carbon fiber-reinforced polymer plates, J. Compos. Constr. 8 (2) (2004) 163–172.
[4] X.L. Zhao, L. Zhang, State-of-the-art review on FRP strengthened steel structures, Eng. Struct. 29 (8) (2007) 1808–1823.
[5] K.A. Harries, A.J. Peck, E.J. Abraham, Enhancing stability of structural steel sections using FRP, Thin-Walled Struct. 47 (10) (2009) 1092–1101.
[6] E.C. Karam, R.A. Hawileh, T. El Maaddawy, J.A. Abdalla, Experimental investigations of repair of pre-damaged steel-concrete composite beams using CFRP laminates and mechanical anchors, Thin-Walled Struct. 112 (2017) 107–117.
[7] M. Madhavan, V. Sanap, R. Verma, S. Selvaraj, Flexural strengthening of structural steel angle sections using CFRP: experimental investigation, J. Compos. Constr. 20 (1) (2015), 04015018.
[8] S. Selvaraj, M. Madhavan, S.U. Dongre, Experimental studies on strength and stiffness enhancement in CFRP-strengthened structural steel channel sections under flexure, J. Compos. Constr. 20 (6) (2016), 04016042.
[9] L.C. Hollaway, P.R. Head, Advanced Polymer Composites and Polymers in the Civil Infrastructure, Elsevier, Oxford, 2001.
[10] L.C. Hollaway, J. Cadei, Progress in the technique of upgrading metallic structures with advanced polymer composites, Prog. Struct. Eng. Mater. 4 (2) (2002) 131–148.
[11] A. Shaat, D. Schnerch, A. Fam, S. Rizkalla, Retrofit of steel structures using fiber-reinforced polymers (FRP): state-of-the-art, in: Presented at Transportation Research Board (TRB) Annual Meeting, 2004 (Washington, DC).
[12] NRC (National Research Council), Guidelines for the Design and Construction of Externally Bonded FRP Systems for Strengthening Existing Structures—Metallic Structures (Preliminary Study). CNR-DT 202/2005, National Research Council Advisory Committee on Technical Recommendations for Construction, Rome, Italy, 2007.
[13] ACI (American Concrete Institute), Guide for the design and construction of externally bonded FRP systems for strengthening concrete structures, ACI 440 (2017), 2R-17, (Farmington Hills, MI).
[14] J.G. Teng, T. Yu, D. Fernando, Strengthening of steel structures with fiber-reinforced polymer composites, J. Constr. Steel Res. 78 (2012) 131–143.
[15] J.M. Sena Cruz, J.A. Barros, R. Gettu, A.F. Azevedo, Bond behavior of near-surface mounted CFRP laminate strips under monotonic and cyclic loading, J. Compos. Constr. 10 (4) (2006) 295–303.
[16] R. Seracino, N.M. Jones, M.S.M. Ali, M.W. Page, D.J. Oehlers, Bond strength of near-surface mounted FRP strip-to-concrete joints, J. Compos. Constr. 11 (4) (2007) 401–409.
[17] J.G. Teng, Y.M. Hu, Behaviour of FRP-jacketed circular steel tubes and cylindrical shells under axial compression, Constr. Build. Mater. 21 (4) (2007) 827–838.
[18] E. Ghafoori, M. Motavalli, Lateral-torsional buckling of steel I-beams retrofitted by bonded and un-bonded CFRP laminates with different pre-stress levels: experimental and numerical study, Constr. Build. Mater. 76 (2015a) 194–206.
[19] E. Ghafoori, M. Motavalli, Normal, high and ultra-high modulus carbon fiber-reinforced polymer laminates for bonded and un-bonded strengthening of steel beams, Mater. Des. 67 (2015b) 232–243.
[20] E. Ghafoori, M. Motavalli, A. Nussbaumer, A. Herwig, G.S. Prinz, M. Fontana, Design criterion for fatigue strengthening of riveted beams in a 120-year-old railway metallic bridge using pre-stressed CFRP plates, Compos. B Eng. 68 (2015) 1–13.
[21] S. Selvaraj, M. Madhavan, Enhancing the structural performance of steel channel sections by CFRP strengthening, Thin-Walled Struct. 108 (2016) 109–121.
[22] S. Selvaraj, M. Madhavan, Strengthening of unsymmetrical open channel built-up beams using CFRP, Thin-Walled Struct. 119 (2017a) 615–628.
[23] S. Selvaraj, M. Madhavan, CFRP strengthened steel beams: improvement in failure modes and performance analysis, Structure 12 (2017b) 120–131. Elsevier.
[24] E. Ghafoori, A. Hosseini, R. Al-Mahaidi, X.L. Zhao, M. Motavalli, Prestressed CFRP-strengthening and long-term wireless monitoring of an old roadway metallic bridge, Eng. Struct. 176 (2018) 585–605.
[25] S. Selvaraj, M. Madhavan, Strengthening of laterally restrained steel beams subjected to flexural loading using low modulus CFRP: experimental assessment, J. Perform. Constr. Facil. (2019a), https://doi.org/10.1061/(ASCE)CF.1943-5509.0001293.
[26] S. Selvaraj, M. Madhavan, Design of steel beams strengthened with low-modulus CFRP laminates, J. Compos. Constr. 24 (1) (2019b), https://doi.org/10.1061/(ASCE)CC.1943-5614.0000983.
[27] D. Schnerch, M. Dawood, S. Rizkalla, E. Sumner, Proposed design guidelines for strengthening of steel bridges with FRP materials, Constr. Build. Mater. 21 (5) (2007) 1001–1010.
[28] D. Schnerch, S. Rizkalla, Flexural strengthening of steel bridges with high modulus CFRP strips, J. Bridge Eng. 13 (2) (2008) 192–201.
[29] IS 808, Dimensions for hot rolled steel beam, column, channel and angle sections." Bureau of Indian Standards (BIS), 1989.
[30] IS 800, Code of practice for general construction in steel." Bureau of Indian Standards (BIS), 2007.

[31] HCU 232, "Technical Data Sheet – Carbon Woven Reinforcement Fabric - HinFab™ HCU232 - 230 GSM – Uni-Directional Woven Carbon Fabric". Hindustan Composites Solutions, Hindoostan Mills Ltd, Mumbai, India, 2015.
[32] HCP 200C, "Technical Data Sheet – Carbon Woven Reinforcement Fabric - HinFab™ HCP200C - 200 GSM – Plain Woven Carbon Fabric". Hindustan Composites Solutions, Hindoostan Mills Ltd, Mumbai, India, 2015.
[33] P. Feng, Y. Zhang, Y. Bai, L. Ye, Combination of bamboo filling and FRP wrapping to strengthen steel members in compression, J. Compos. Constr. 17 (3) (2013a) 347–356.
[34] P. Feng, Y. Zhang, Y. Bai, L. Ye, Strengthening of steel members in compression by mortar-filled FRP tubes, Thin-Walled Struct. 64 (2013b) 1–12.
[35] ASTM, Standard Test Methods for Tension Testing of Metallic Materials, ASTM International, West Conshohocken, USA, 2013. E8/E8M-13a.
[36] ASTM, Standard Test Method for Tensile Properties of Polymer Matrix Composite Materials, ASTM International, West Conshohocken, PA, 2014. ASTM D3039/D3039M-14.
[37] ASTM, Standard Test Methods for Constituent Content of Composite Materials, ASTM International, West Conshohocken, PA, 2015. ASTM D3171-15.
[38] A.H. Mattock, Flexural strength of prestressed concrete sections by programmable calculator, PCI J. 24 (1) (1979) 32–54.
[39] N. Plevris, T.C. Triantafillou, D. Veneziano, Reliability of RC members strengthened with CFRP laminates, J. Struct. Eng. 121 (7) (1995) 1037–1044.
[40] A.M. Okeil, S. El-Tawil, M. Shahawy, Flexural reliability of reinforced concrete bridge girders strengthened with carbon fiber-reinforced polymer laminates, J. Bridge Eng. 7 (5) (2002) 290–299.
[41] A.H. Zureick, R.M. Bennett, B.R. Ellingwood, Statistical characterization of fiber-reinforced polymer composite material properties for structural design, J. Struct. Eng. 132 (8) (2006) 1320–1327.
[42] M.R. Bambach, H.H. Jama, M. Elchalakani, Axial capacity and design of thin-walled steel SHS strengthened with CFRP, Thin-Walled Struct. 47 (10) (2009) 1112–1121.
[43] N. Wang, B.R. Ellingwood, A.H. Zureick, Reliability-based evaluation of flexural members strengthened with externally bonded fiber-reinforced polymer composites, J. Struct. Eng. 136 (9) (2010) 1151–1160.
[44] C. Galasso, G. Maddaloni, E. Cosenza, Uncertainly analysis of flexural overstrength for capacity design of RC beams, J. Struct. Eng. 140 (7) (2014), 04014037.
[45] N. Wang, B.R. Ellingwood, Limit state design criteria for FRP strengthening of RC bridge components, Struct. Saf. 56 (2015) 1–8.
[46] American Association of State Highway and Transportation Officials (AASHTO), LRFD Bridge Design Specifications, 2004 (Washington, D.C).
[47] A.S. Nowak, M.M. Szerszen, Calibration of design code for buildings (ACI 318): Part 1-statistical models for resistance, ACI Struct. J. 100 (3) (2003) 377–382.
[48] M.M. Szerszen, A.S. Nowak, Calibration of design code for buildings (ACI 318): Part 2-reliability analysis and resistance factors, ACI Struct. J. 100 (3) (2003) 383–391.

Further reading

[49] A. Hosseini, E. Ghafoori, R. Al-Mahaidi, X.L. Zhao, M. Motavalli, Strengthening of a 19th-century roadway metallic bridge using nonprestressed bonded and prestressed unbonded CFRP plates, Constr. Build. Mater. 209 (2019) 240–259.
[50] S. Selvaraj, M. Madhavan, Retrofitting of structural steel channel sections using cold-formed steel encasing channels, J. Perform. Constr. Facil. 32 (4) (2018), 04018049.